



Melatonin acts synergistically with pazopanib against renal cell carcinoma cells through p38 mitogen-activated protein kinase-mediated mitochondrial and autophagic apoptosis

Chien-Pin Lai^{1,*}, Yong-Syuan Chen^{2,*}, Tsung-Ho Ying^{3,4}, Cheng-Yen Kao⁵, Hui-Ling Chiou⁶, Shao-Hsuan Kao^{2,6}, Yi-Hsien Hsieh^{2,6}

¹Division of Nephrology, Department of Medicine, Chung-Kang Branch, Cheng Ching General Hospital, Taichung City, Taiwan

²Institute of Medicine, Chung Shan Medical University, Taichung City, Taiwan

³Department of Obstetrics and Gynecology, College of Medicine, Chung Shan Medical University, Taichung City, Taiwan

⁴Department of Obstetrics and Gynecology, Chung Shan Medical University Hospital, Taichung City, Taiwan

⁵Institute of Microbiology and Immunology, College of Life Sciences, National Yang Ming Chiao Tung University, Taipei, Taiwan

⁶Department of Medical Research, Chung Shan Medical University Hospital, Taichung City, Taiwan

Background: Mounting evidence indicates that melatonin has possible activity against different tumors. Pazopanib is an anticancer drug used to treat renal cell carcinoma (RCC). This study tested the anticancer activity of melatonin combined with pazopanib on RCC cells and explored the underlying mechanistic pathways of its action.

Methods: The 786-O and A-498 human RCC cell lines were used as cell models. Cell viability and tumorigenesis were detected with the MTT and colony formation assays, respectively. Apoptosis and autophagy were assessed using TUNEL, annexin V/propidium iodide, and acridine orange staining with flow cytometry. The expression of cellular signaling proteins was investigated with western blotting. The *in vivo* growth of tumors derived from RCC cells was evaluated using a xenograft mouse model.

Results: Together, melatonin and pazopanib reduced cell viability and colony formation and promoted the apoptosis of RCC cells. Furthermore, the combination of melatonin and pazopanib triggered more mitochondrial, caspase-mediated, and LC3-II-mediated autophagic apoptosis than melatonin or pazopanib alone. The combination also induced higher activation of the p38 mitogen-activated protein kinase (p38MAPK) in the promotion of autophagy and apoptosis by RCC cells than melatonin or pazopanib alone. Finally, tumor xenograft experiments confirmed that melatonin and pazopanib cooperatively inhibited RCC growth *in vivo* and predicted a possible interaction between melatonin/pazopanib and LC3-II.

Conclusion: The combination of melatonin and pazopanib inhibits the growth of RCC cells by inducing p38MAPK-mediated mitochondrial and autophagic apoptosis. Therefore, melatonin might be a potential adjuvant that could act synergistically with pazopanib for RCC treatment.

Keywords: Apoptosis, Autophagy, Melatonin, Pazopanib, Renal cell carcinoma

Received: June 3, 2022; **Revised:** September 26, 2022; **Accepted:** September 27, 2022

Correspondence: Shao-Hsuan Kao

Institute of Medicine, Chung Shan Medical University, No. 110, Sec. 1, Jianguo N. Rd., Taichung City 40201, Taiwan. E-mail: kaosh@csmu.edu.tw
ORCID: <https://orcid.org/0000-0002-4929-3858>

Yi-Hsien Hsieh

Institute of Medicine, Chung Shan Medical University, No. 110, Sec. 1, Jianguo N. Rd., Taichung City 40201, Taiwan. E-mail: hyhsien@csmu.edu.tw
ORCID: <https://orcid.org/0000-0003-4942-1888>

*Chien-Pin Lai and Yong-Syuan Chen contributed equally to this article as co-first authors.

Copyright © 2023 by The Korean Society of Nephrology

© This is an Open Access article distributed under the terms of the Creative Commons Attribution Non-Commercial and No Derivatives License (<http://creativecommons.org/licenses/by-nc-nd/4.0/>) which permits unrestricted non-commercial use, distribution of the material without any modifications, and reproduction in any medium, provided the original works properly cited.

Introduction

Renal cell carcinoma (RCC) is the most lethal of the urinary cancers; it is generally asymptomatic and highly metastatic, and it shows a poor response to chemotherapy in the late stage [1,2]. The histological cell types of RCC are clear cell RCC, papillary RCC, chromophobe RCC, and collecting duct RCC [3], and each of those types has different genetic and tumorigenic properties. Clear cell RCC comprises 75% to 80% of RCC cases, and papillary RCC and chromophobe RCC comprise most of the other 25%. Collecting duct RCC is rare, comprising <1 % of RCC cases [3]. Resection surgery is commonly performed for localized RCC; however, RCC has high recurrence rates of 20% to 40% after nephrectomy and high frequency of drug resistance, resulting in high mortality rates among advanced RCC patients [4,5].

Recently, the introduction of targeted molecular therapies has markedly improved the prognosis for advanced RCC patients. These targeted therapies include the mammalian target of rapamycin (mTOR) inhibitors, antiangiogenic antibody, and tyrosine kinase inhibitors (TKIs). Pazopanib, a TKI used for RCC treatment, inhibits vascular endothelial growth factor receptor (VEGFR)-mediated angiogenesis and receptor tyrosine kinase (RTK)-induced cell growth *in vivo* [6,7]. In the absence of *in vivo* microenvironments and interactions among cancer cells, immune cells, and vascular cells, TKIs can directly affect RCC cells through their pharmacologic characteristics, but assessing the *in vitro* action of TKIs in single cancer cell models remains challenging. Therefore, few studies have explored the *in vitro* effects of TKIs on individual RCC cells [8,9].

Melatonin (N-acetyl-5-methoxytryptamine) is an indole amine mainly produced by the pineal gland in response to darkness, and it is a pleiotropic molecule with various biological activities [10]. Mounting evidence collected during the past few decades suggests that melatonin has diverse physiological roles in humans and can modulate many pathways, including those related to oxidative stress, immune modulation, and hematopoiesis [11,12]. In parallel, an increasing number of studies have shown that melatonin exerts anticancer and tumor-suppressing effects through various mechanisms [13,14]. Importantly, it was found that combining melatonin with anticancer therapy could enhance conventional treatments and reduce side effects [15,16]. However, whether melatonin synergistically

acts with pazopanib in its antitumor activity against RCC has not been fully explored. In this study, we investigated the anticancer activity of melatonin combined with pazopanib in RCC cells by evaluating the inhibitory effects of their combination on cell viability, colony formation, and *in vivo* tumor growth. We demonstrate that they induce apoptosis and autophagy and explicate the mechanistic cascade behind their effects. Our findings provide evidence that melatonin acts cooperatively with pazopanib to inhibit tumorigenesis by RCC cells.

Methods

Reagents and antibodies

Melatonin (Supplementary Fig. 1A, available online), Giemsa solution, and MTT were purchased from Sigma-Aldrich. Pazopanib was purchased from Cayman Chemical. Fetal bovine serum (FBS) and penicillin/streptomycin were purchased from HyClone. Doramapimod (BIRB 796) was purchased from Merck Millipore. Z-VAD-FMK was purchased from BioVision. Western blotting antibodies against cleaved-caspase-3 (#9668), cleaved-caspase-9 (#9508), cleaved-poly (ADP-ribose) polymerase (PARP) (#9542), and Bax (#5023) were purchased from Cell Signaling Technology. Antibodies against phospho-p38 mitogen-activated protein kinase (p38MAPK; sc-166182), p38MAPK (sc-7972), Bcl-2 (sc-492), cytochrome c (sc-13156), β -actin (sc-69879), and small inhibitory RNA-LC3-II (LC3-II siRNA; sc-43390) were purchased from Santa Cruz Biotechnology. Antibodies against p62 (NBP 1-48320) and LC3-II (NB 100-2220) were purchased from Novus Biologicals. Secondary goat anti-rabbit immunoglobulin G (IgG) and goat anti-mouse IgG antibodies were purchased from Merck Millipore.

Cell culture

The 786-O (BCRC-60243) and A-498 (BCRC-60241) human RCC cell lines were purchased from the Bioresources Collection and Research Center, Food Industry Research and Development Institute (Hsinchu, Taiwan). Cells were grown in RPMI-1640 (786-O) or Eagle's MEM (A-498) supplemented with 1% penicillin/streptomycin and sodium bicarbonate and 10% (v/v) FBS at 37 °C in a humidified incubator at 5% CO₂. Subculture was performed when the

cells reached 80% confluence.

Cell viability assay

Cell viability was determined using the MTT assay as previously described [17]. Briefly, 2×10^4 cells were seeded into a 6-well plate and treated with melatonin at 1, 2, 4, 6, or 8 mM; pazopanib at 1, 2, 5, 7.5, or 10 μ M; or melatonin (4 mM) combined with pazopanib (5 μ M) for 24 or 48 hours. Then the cells were incubated with the MTT (0.5 mg/mL) solution. After adding isopropanol to solubilize the formed formazan, we measured the absorbance of the solution at 570 nm using a Multiskan MS ELISA reader (Labsystems). The percentage of viable cells was estimated by comparing the test results with those from untreated control cells.

Colony formation assay

The 786-O and A-498 cells (2×10^3 per well) were seeded in six-well plates and treated with the drugs for 1 week. The colonies were then stained with phosphate-buffered saline (PBS) containing 5% v/v Giemsa solution overnight at room temperature. At the end of the incubation, the cell colonies were fixed with methanol, stained with 5% Giemsa solution, and photographed using a Nikon Eclipse TE2000-U microscope equipped with a Nikon DXM1200 digital camera. Then the blue colonies were calculated and illustrated.

Annexin V/propidium iodide assay and measurement of the mitochondrial membrane potential

The 786-O and A-498 cells (2×10^5) were seeded in 6-cm dishes and treated with melatonin, pazopanib, or both for 48 hours. Annexin V/propidium iodide (PI) staining and the mitochondrial membrane potential were detected using a Muse annexin V and dead cell assay kit and a Muse Mitopotential assay kit (Millipore), respectively. Then, the cells were analyzed using a Muse cell analyzer (Millipore).

TUNEL staining

The 786-O (1×10^4 cells/well) and A-498 (5×10^3 cells/well) cells were cultured on eight-well Lab-Tek chambered cover-glass (Thermo) and treated with melatonin (4 mM) and

pazopanib (5 μ M) alone or together at 37 °C for 24 hours. Then, the cells were washed with PBS, fixed for 60 minutes with 4% paraformaldehyde, permeabilized for 5 minutes with PBS containing 0.1% Triton X-100 on ice, and stained using an *in situ* cell death detection kit. DAPI (4',6-diamidino-2-phenylindole) reagent was used to mark the cell nuclei. The data were visualized using a Zeiss LSM 510 META confocal microscope.

Detection of acridine orange

After seeding and drug treatment, cells were stained with 1- μ g/mL acridine orange (AO) reagent in fresh medium for 30 minutes in a 37 °C incubator. Then, the cells were immediately collected and analyzed with a FACScan flow cytometer (BD Biosciences).

Western blotting

Western blotting was performed as previously described [18]. Briefly, cells were lysed in RIPA buffer containing a protease and phosphatase inhibitor cocktail (Sigma-Aldrich). The resulting crude proteins were separated using sodium dodecyl sulfate-polyacrylamide gel electrophoresis, transferred to polyvinylidene difluoride membranes (Immobilon; Merck), and reacted with first the primary antibodies and then the secondary antibodies. The bound antibodies were detected using enhanced chemiluminescence reagent (SuperSignal West Dura HRP detection kit; Pierce Biotechnology) and an image analysis system (Fujifilm). A densitometric analysis was performed for semi-quantitation of the chemiluminescent signals.

Knockdown of LC3-II by siRNA

LC3-II expression knockdown was conducted using specific siRNAs according to the manufacturer's instructions. Briefly, cells were transfected with LC3-II siRNA (200 nM; Santa Cruz Biotechnology) using Lipofectamine RNAi MAX (Invitrogen) at 37 °C and 5% CO₂ for 72 hours; treated with melatonin, pazopanib, or both; and then collected for subsequent analyses.

In vivo assessment of xenograft tumor growth

Xenografts were placed in 5-week-old male BALB/c-nude mice obtained from the National Laboratory Animal Center (Taipei, Taiwan). During the experiments, the mice were maintained in cages with a regular 12-hour light/dark cycle and fed *ad libitum* with a standard diet. All the experimental protocols were approved by the Institutional Animal Ethics Committee of Chung Shan Medical University (No. 2715). The mice received daily treatments of melatonin (100 mg/kg, prepared in PBS) via oral gavage, pazopanib (100 mg/kg) via oral gavage, or both. After drug administration, 786-O cells (5×10^6) were subcutaneously injected into the right flanks of the mice ($n = 5$ per group). Tumor volumes were measured with calipers and calculated according to the following formula: tumor volume = (length \times width²)/2. The body weights and tumor volumes of the mice were determined on days 3, 7, 10, 14, 17, 21, 24, and 28. After 4 weeks, the mice were sacrificed in a CO₂ chamber, and the tumor nodules were acquired and recorded.

Molecular docking approach

The binding mode and selectivity of melatonin and pazopanib for LC3 were analyzed using AutoDock Vina 4.0 (Trott and Olson 2010), which required the ligand and receptor in PDBqt format and the configuration file in txt format. The structure of LC3 was downloaded from National Center for Biotechnology Information (NCBI) PubChem (CID: 6918774). Pymol was used to verify the presence or absence of hydrogen, the stereochemistry of chiral carbons, number of rotatable bonds, and number of hydrogen acceptors and donors. The Gasteiger charge was designated, and the torsions for melatonin and pazopanib were permitted to rotate during the docking procedure by using AutoDock tools version 1.5.6. The ligands were saved in PDBqt format. The receptor was prepared in AutoDock tools version 1.5.6: polar hydrogens were assigned to the receptor, the grid-box was centered on LC3, and the dimensions were set to 30, 30, 30 Å (x, y, z) to contain all the active site residues within the box. The receptor was saved in PDBqt format.

Statistical analysis

The data from three independent experiments are present-

ed as the mean \pm standard deviation unless indicated otherwise. Student t test was used to analyze the significance of differences. Results with p-values of <0.05 were considered to be statistically significant.

Results

Melatonin combined with pazopanib enhances activity against human renal cell carcinoma cells

The effects of melatonin on cell viability were tested first, and the results showed that 24- or 48-hour treatments of melatonin significantly reduced the viability of 786-O and A-498 cells in a dose-dependent manner (4–8 mM, $p < 0.01$ compared with control) (Supplementary Fig. 1B, available online). In addition, melatonin remarkably diminished the colony formation of both RCC cell lines (6 and 8 mM, $p < 0.01$ compared with control) (Supplementary Fig. 1C, available online). Next, we evaluated whether the reduced viability of the RCC cells resulted from apoptosis. By using annexin V/PI staining, we observed that melatonin dose-dependently induced apoptosis in up to $36.8\% \pm 4.1\%$ and $43.8\% \pm 1.1\%$ of 786-O and A-498 RCC cells, respectively ($p < 0.01$ compared with control) (Supplementary Fig. 1D, available online). Consistently, we also found that melatonin contributed to PARP cleavage (Supplementary Fig. 1E, available online).

We next evaluated the cytotoxicity of pazopanib to RCC cells. After 24 hours of pazopanib (1–10 μ M) treatment, the viability of 786-O and A-498 cells was not significantly affected compared with the control at $\leq 7.5 \mu$ M (Fig. 1A). Similar results were observed in response to 48-hour treatment. Among the tested concentrations of pazopanib, only the highest, 10- μ M pazopanib, reduced the viability of both RCC cell lines to approximately 75% of the control ($p < 0.05$ compared with control). When we explored the anti-tumorigenicity of a combination of 4-mM melatonin and 5- μ M pazopanib on RCC cells, we found that it reduced the viability of the RCC cells to near 45% (24-hour treatment) of the control ($p < 0.01$) (Fig. 1B). Similarly, melatonin and pazopanib together exhibited a synergistic inhibitory effect on the colony formation capability of 786-O and A-498 cells ($p < 0.01$ compared with melatonin or pazopanib alone) (Fig. 1C).

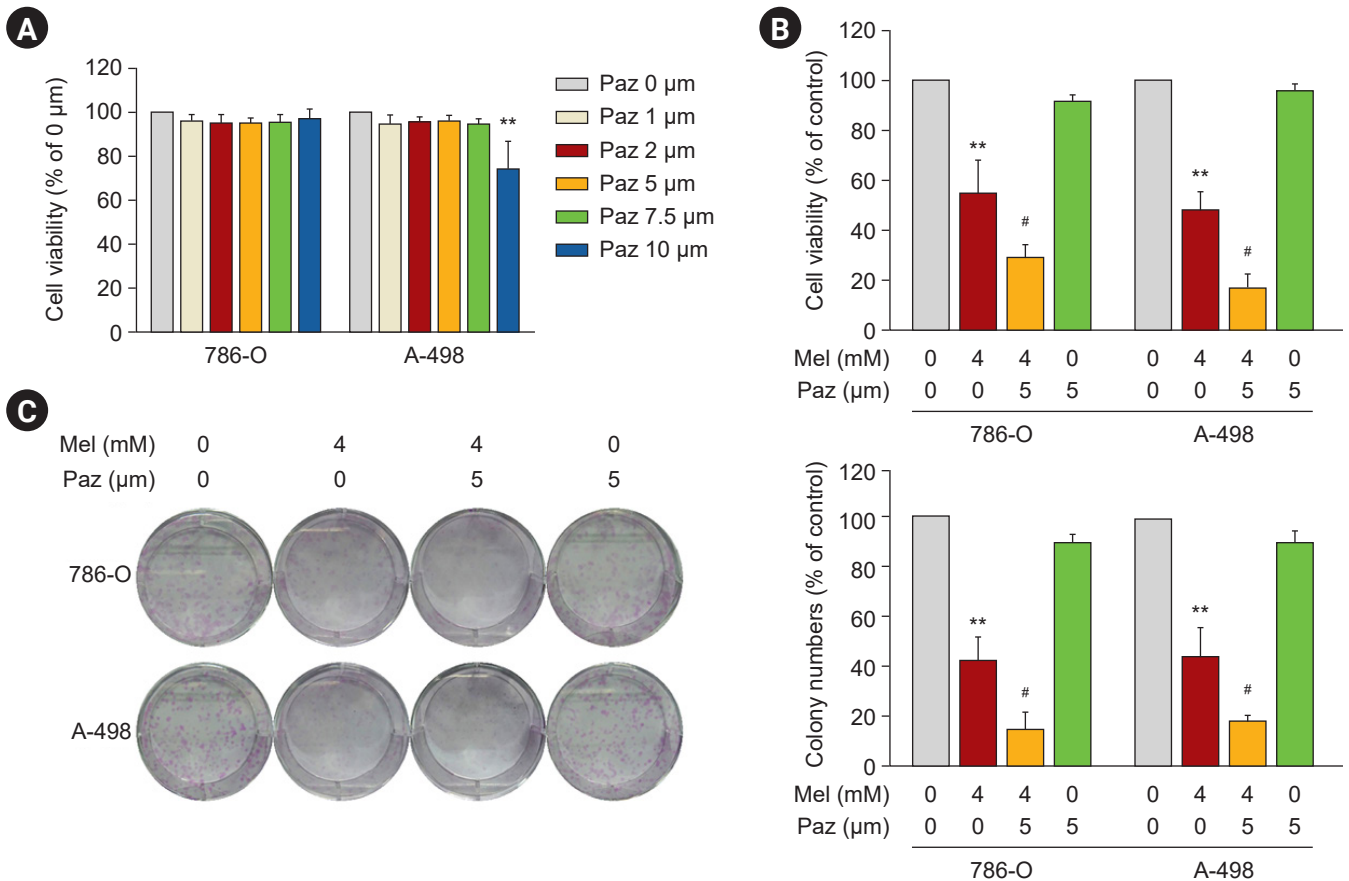


Figure 1. Melatonin (Mel) cooperatively promotes the antitumoral activity of pazopanib (Paz) against human 786-O and A-498 renal cell carcinoma cells. (A) Cells were treated with Paz at serial concentrations for 24 hours and then subjected to a cell viability assay. Cells were treated with 4-mM Mel, 5- μM Paz, or their combination for 24 hours, and then subjected to (B) a cell viability assay or (C) a colony formation assay. Cell viability is presented as a percentage of the control.

** $p < 0.01$ compared with the control; # $p < 0.05$ compared with the combination.

Melatonin combined with pazopanib synergistically promotes apoptosis and activates a caspase cascade in renal cell carcinoma cells

Next, we explored the mechanism of the decline in cell viability. As shown in Fig. 2A, the combination of 4-mM melatonin and 5- μM pazopanib induced significantly more apoptosis in 786-O and A-498 cells than melatonin or pazopanib alone ($p < 0.01$). Consistently, the combination of melatonin and pazopanib induced more apoptotic signaling cascades (caspase-9, caspase-3, and PARP cleavage) in 786-O and A-498 cells than melatonin or pazopanib alone (Fig. 2B). Our results in the TUNEL staining assay were consistent with those observed in western blotting (Fig. 2C). We thus explored the role of caspases in the apoptosis

induced by the combination of melatonin and pazopanib. As shown in Fig. 2D, pretreatment with a caspase inhibitor, Z-VAD, significantly attenuated the apoptosis induced by the combination of melatonin and pazopanib ($p < 0.05$). Together, these results show that melatonin synergistically enhanced the apoptosis induced by pazopanib by promoting a caspase-mediated cascade.

Melatonin combined with pazopanib induces the depolarization of mitochondria and a Bax/Bcl-2 imbalance in renal cell carcinoma cells

We next elucidated the involvement of the mitochondrial pathway. As shown in Fig. 3A, melatonin increased the number of cells with depolarized mitochondria by 29.3% \pm

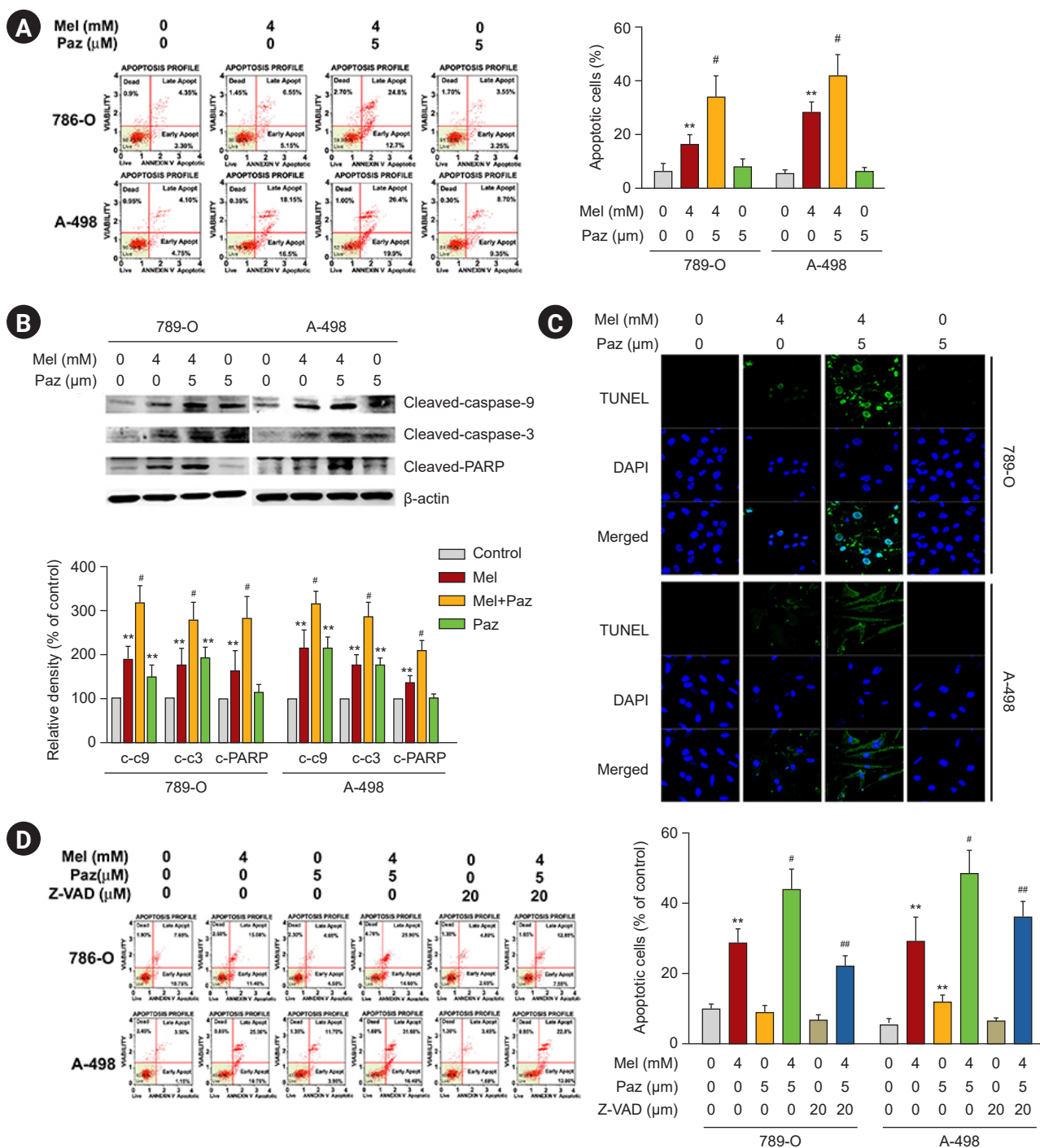


Figure 2. Melatonin (Mel) combined with pazopanib (Paz) synergistically promotes caspase-dependent apoptosis in human 786-O and A-498 renal cell carcinoma cells. Cells were treated with 4-mM Mel, 5-μM Paz, or their combination for 24 hours and then subjected to (A) an annexin V/propidium iodide (PI)-flow cytometric analysis or (B) western blotting to evaluate cellular apoptosis. (C) TUNEL-positive cells are presented as green-stained nuclei, with DAPI (4',6-diamidino-2-phenylindole) as the nucleus marker (×100). (D) Cells were pretreated with Z-VAD (BioVision) for 1 hour, treated with 4-mM Mel, 5-μM Paz, or their combination for 24 hours, and then subjected to (A) an annexin V/PI-flow cytometric analysis to evaluate cellular apoptosis. Apoptotic cells are presented as a percentage of the control.

PARP, poly (ADP-ribose) polymerase.

**p < 0.01 compared with the control; #p < 0.05 and ##p < 0.01 compared with the combination

1.8% (786-O) and $28.6\% \pm 2.1\%$ (A-498), compared with the control ($p < 0.01$). The combination of melatonin and pazopanib further increased mitochondria depolarization in RCC cells to $42.2\% \pm 4.6\%$ (786-O) and $40.9\% \pm 2.2\%$ (A-498) ($p < 0.05$ compared with melatonin or pazopanib alone). On the contrary, pazopanib insignificantly affected mitochondria depolarization in RCC cells. Similarly, melatonin alone significantly elevated the Bax/Bcl-2 ratio, whereas pazopanib alone had no effect on the Bax/Bcl-2 ratio in RCC cells. Notably, melatonin combined with pazopanib increased the Bax/Bcl-2 ratio and level of cytochrome c in RCC cells by more than melatonin or pazopanib alone ($p < 0.05$) (Fig. 3B).

Melatonin combined with pazopanib promotes autophagic apoptosis in renal cell carcinoma cells

Subsequently, we explored the role of autophagy in the

effects of melatonin, pazopanib, and their combination on RCC cells. As shown in Fig. 4A, the AO staining assay revealed that melatonin increased AO intensity in 786-O and A-498 cells, and melatonin combined with pazopanib synergistically elevated AO intensity in RCC cells ($p < 0.05$ compared with melatonin or pazopanib alone). We next examined the effects of melatonin and pazopanib on LC3-II and p62, which are important autophagy markers. As shown in Fig. 4B, melatonin increased the LC3-II level in 786-O and A-498 cells, and melatonin combined with pazopanib synergistically elevated the LC3-II level in RCC cells. In contrast, melatonin decreased the p62 level in 786-O and A-498 cells, and melatonin combined with pazopanib further lowered the p62 level in the RCC cells. Then, we elucidated the role of autophagy in the apoptosis of RCC cells following treatment with melatonin and pazopanib. As shown in Fig. 4C, the synergistic effects of combining melatonin and pazopanib on inducing apoptosis in 786-

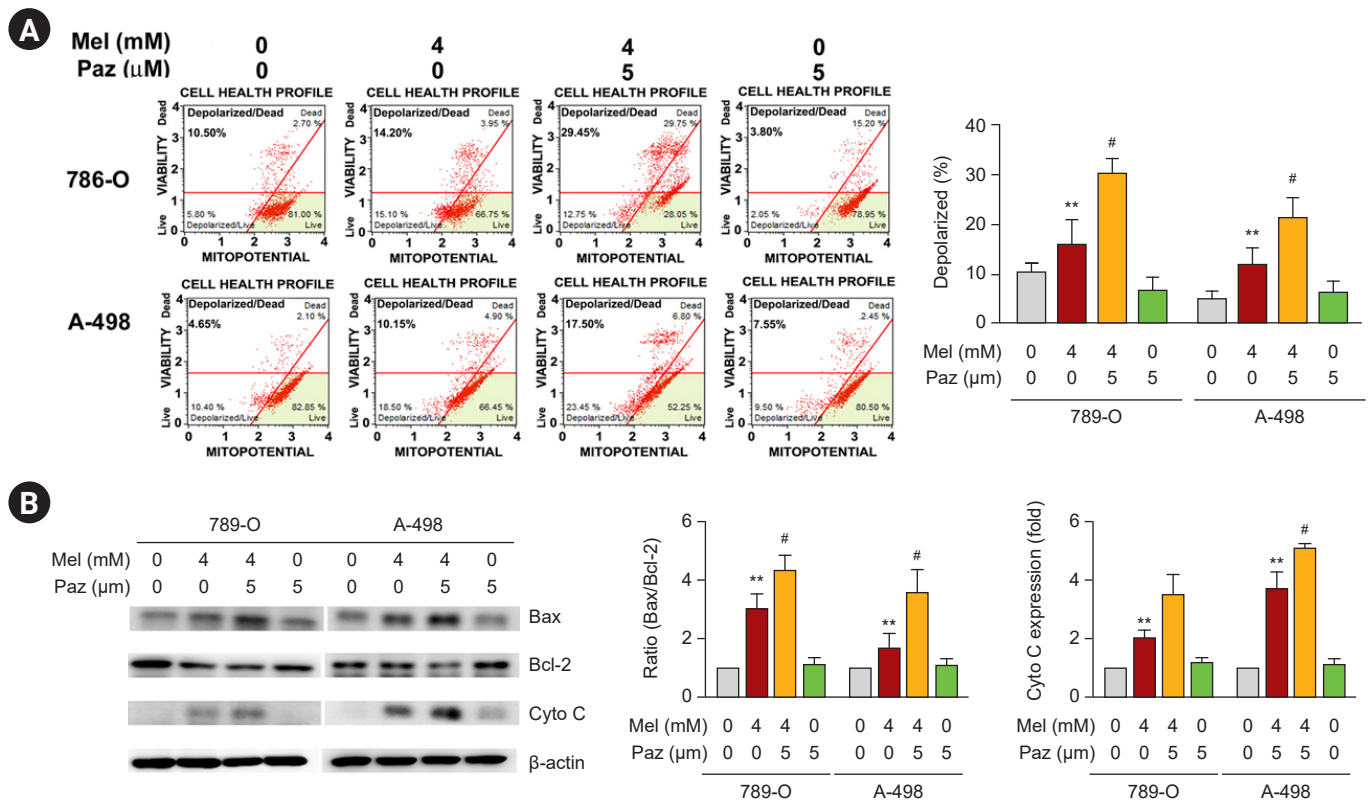


Figure 3. Melatonin (Mel) combined with pazopanib (Paz) potentiates mitochondrial apoptosis in human 786-O and A-498 renal cell carcinoma cells. Cells were treated with 4-mM Mel, 5- μ M Paz, or their combination for 24 hours and then subjected to (A) a mitochondrial membrane potential assay, or (B) western blotting to evaluate mitochondrial apoptotic signals. Depolarized cells are presented as a percentage of the control.

** $p < 0.01$ compared with the control; # $p < 0.05$ compared with Mel alone.

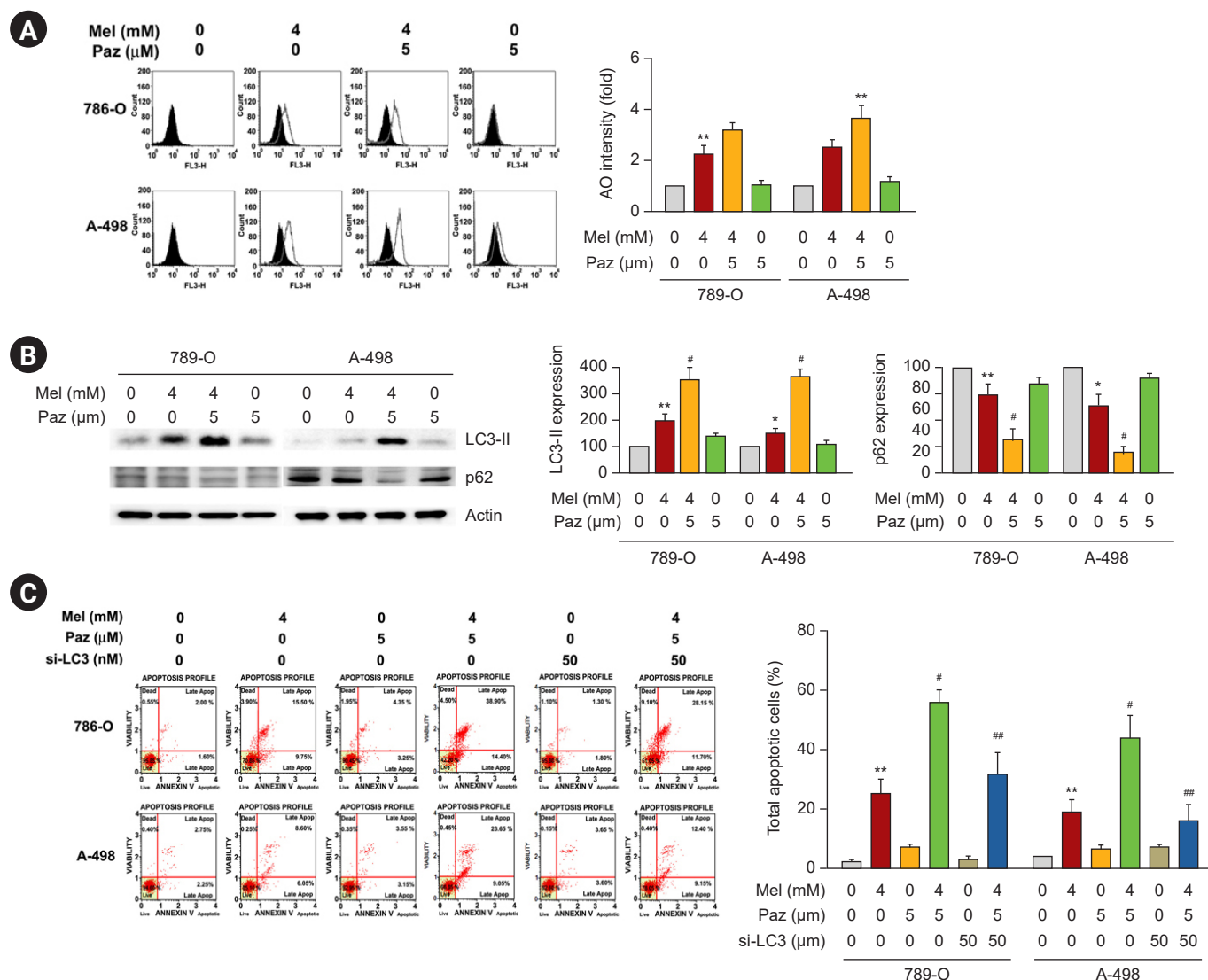


Figure 4. Melatonin (Mel) combined with pazopanib (Paz) induces autophagy-mediated apoptosis in human 786-O and A-498 renal cell carcinoma cells. Cells were treated with 4-mM Mel, 5-μM Paz, or their combination for 24 hours and then subjected to (A) an AO staining assay, or (B) western blotting to evaluate autophagic signals. (C) Cells were pretreated with specific small inhibitory RNA against LC3-II (si-LC3-II); treated with 4-mM Mel, 5-μM Paz, or their combination for 24 hours; and then subjected to an annexin V/propidium iodide-flow cytometric analysis to evaluate cellular apoptosis. Apoptotic cells are presented as a percentage of the control. ***p* < 0.01 compared with the control. #*p* < 0.05 and ###*p* < 0.01 compared with the combination.

O and A-498 cells were significantly attenuated by LC3-II knockdown (*p* < 0.05).

Involvement of p38MAPK in the induction of mitochondrial and autophagic apoptosis in renal cell carcinoma cells caused by the combination of melatonin and pazopanib

We investigated the involvement of p38MAPK, a signaling

kinase with a key role in tumor-associated angiogenesis [19], in the apoptosis induced by melatonin, pazopanib, and their combination. As shown in Fig. 5A, melatonin and pazopanib individually induced the phosphorylation of p38MAPK, and the combination of melatonin and pazopanib resulted in higher phosphorylation of p38MAPK than melatonin or pazopanib alone. When we used a specific p38MAPK inhibitor, BIRB 796, our results showed that

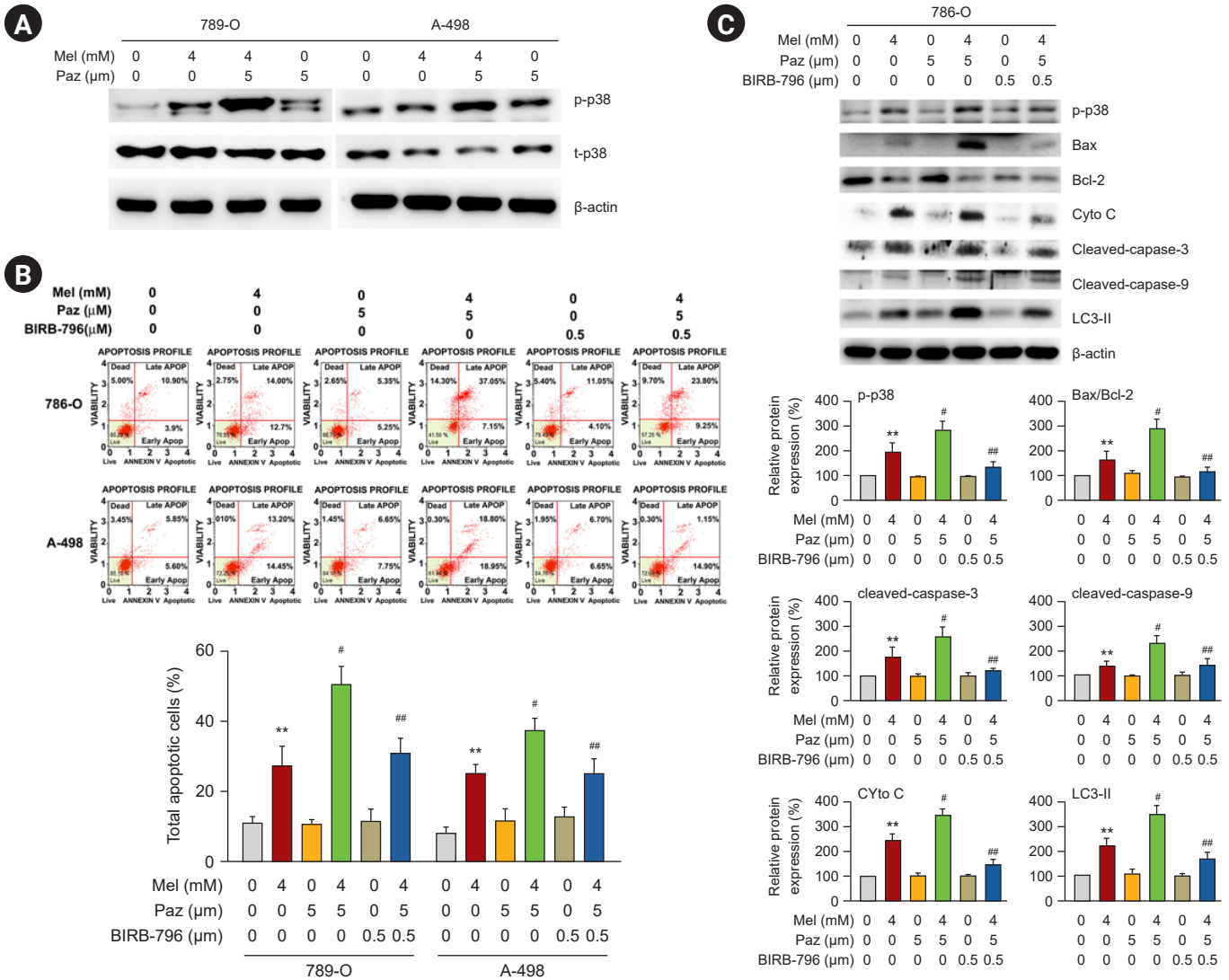


Figure 5. Involvement of p38MAPK in the autophagy-mediated apoptotic cascade induced in human 786-O and A-498 renal cell carcinoma cells by melatonin (Mel) combined with pazopanib (Paz). (A) Cells were treated with 4-mM Mel, 5- μ M Paz, or their combination for 24 hours and then subjected to western blotting for immunodetection of phospho-p38MAPK and total-p38MAPK. (B and C) Cells were pretreated with a specific p38MAPK inhibitor (BIRB 796; Merck Millipore); treated with 4-mM Mel, 5- μ M Paz, or their combination for 24 hours; and then subjected to (B) an annexin V/propidium iodide-flow cytometric analysis to evaluate cellular apoptosis or (C) western blotting for immunodetection of apoptotic and autophagic signaling components. Apoptotic cells are presented as a percentage of the control.

p38MAPK, p38 mitogen-activated protein kinase.

* $p < 0.01$ compared with the control. # $p < 0.05$ and ## $p < 0.01$ compared with the combination.

inhibiting p38MAPK significantly reduced the apoptosis of 786-O and A-498 cells in response to the combined treatment of melatonin and pazopanib ($p < 0.05$) (Fig. 5B). We also explored the effect of p38MAPK inhibition on the mitochondrial and autophagic apoptotic cascade induced by the combination of melatonin and pazopanib. Those find-

ings reveal that p38MAPK inhibition attenuated both the elevated levels of Bax, cytochrome c, caspase-3, caspase-9, and LC3-II and the lowered level of Bcl-2 in 786-O cells exposed to melatonin and pazopanib together (Fig. 5C).

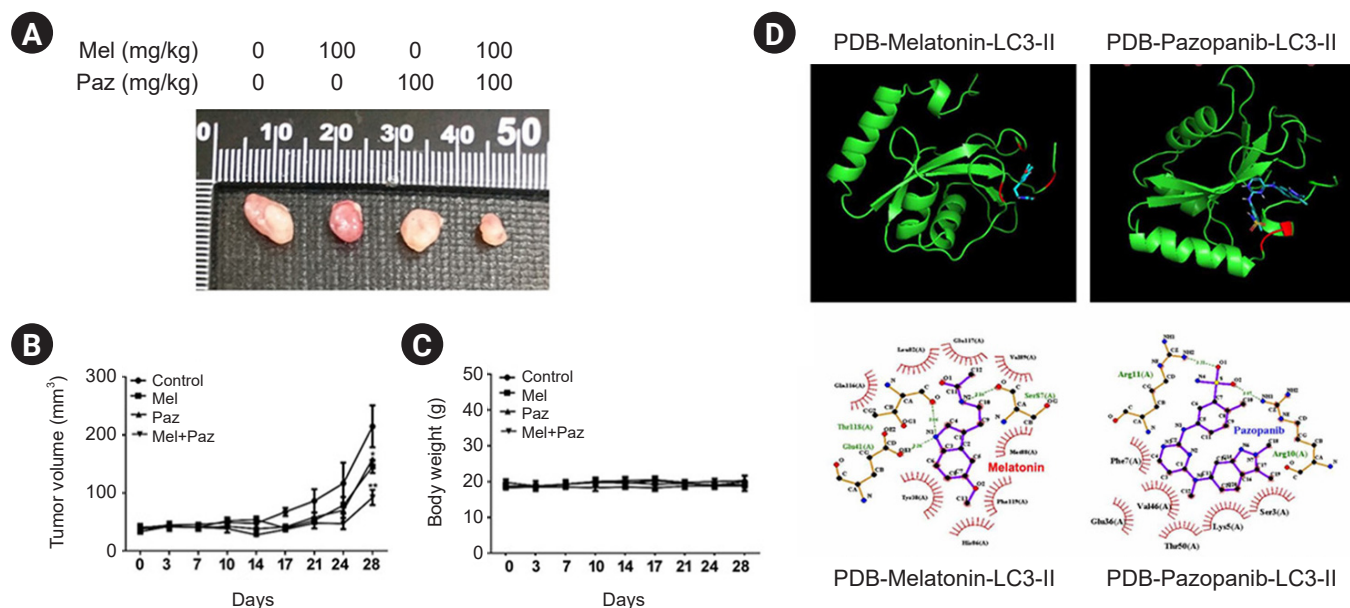


Figure 6. Melatonin (Mel) combined with pazopanib (Paz) reduces *in vivo* tumor growth, and Mel/Paz interact with LC3-II. (A–C) The 786-O cells were inoculated into nude mice, and then Mel (100 mg/kg), Paz (100 mg/kg), or their combination was administered weekly by oral injection, respectively, for 28 days. The tumor volumes and body weights were measured on days 3, 7, 10, 14, 17, 21, 24, and 28. At the end of the experiment, tumors were acquired from the sacrificed mice. * $p < 0.05$ and ** $p < 0.01$, respectively, compared with the control. (D) Molecular docking analysis to examine the binding of Mel and LC3 and the binding of Paz and LC3. The predicted interactions between the amino acids on LC3 and Mel or Paz are indicated.

Melatonin combined with pazopanib cooperatively inhibits tumor growth *in vivo*, and LC3-II interacts with melatonin or pazopanib

The *in vivo* inhibitory effect of melatonin and pazopanib on tumor growth was tested using a xenograft mouse model. As shown in Fig. 6A, B, on the 28th day after the inoculation of 786-O cells, both melatonin and pazopanib alone significantly reduced the tumor volume in mice ($p < 0.05$ compared with control), and the combination of melatonin and pazopanib further reduced tumor volume compared with either treatment alone ($p < 0.01$). In parallel, during the 28 days following the inoculation of 786-O cells, the administration of melatonin, pazopanib, or both did not significantly alter the body weights of the treated mice (Fig. 6C).

Subsequently, we explored the interaction between the LC3-II protein and melatonin or pazopanib using a molecular docking analysis. The predicted hydrogen bonding networks show that the Glu4, Thr315, and Ser57 residues in LC3-II might interact with melatonin through hydrogen bonding (Fig. 6D). In addition, the Arg11 and Arg18 resi-

dues in LC3-II might interact with pazopanib through hydrogen bonding (Fig. 6D). Moreover, potential hydrophobic interactions between melatonin/LC3 and pazopanib/LC3 were also predicted (Fig. 6D). These results indicate that melatonin and pazopanib might interact directly with the LC3 protein.

Discussion

In this study, we explored the antitumor activities of melatonin and pazopanib against RCC cells, and we found that melatonin combined with pazopanib triggers apoptosis of RCC cells in associated with p38MAPK-mediated mitochondrial and autophagic pathways (Fig. 7). These findings provide evidence that melatonin could serve as a potential adjuvant for pazopanib in the treatment of RCC.

Pazopanib is a TKI indicated as a first-line therapy for patients with metastatic RCC [20] because it can selectively inhibit VEGFR-mediated angiogenesis and RTK-promoted tumor growth [21]. Furthermore, pazopanib inhibits all the platelet-derived growth factor receptors subtypes,

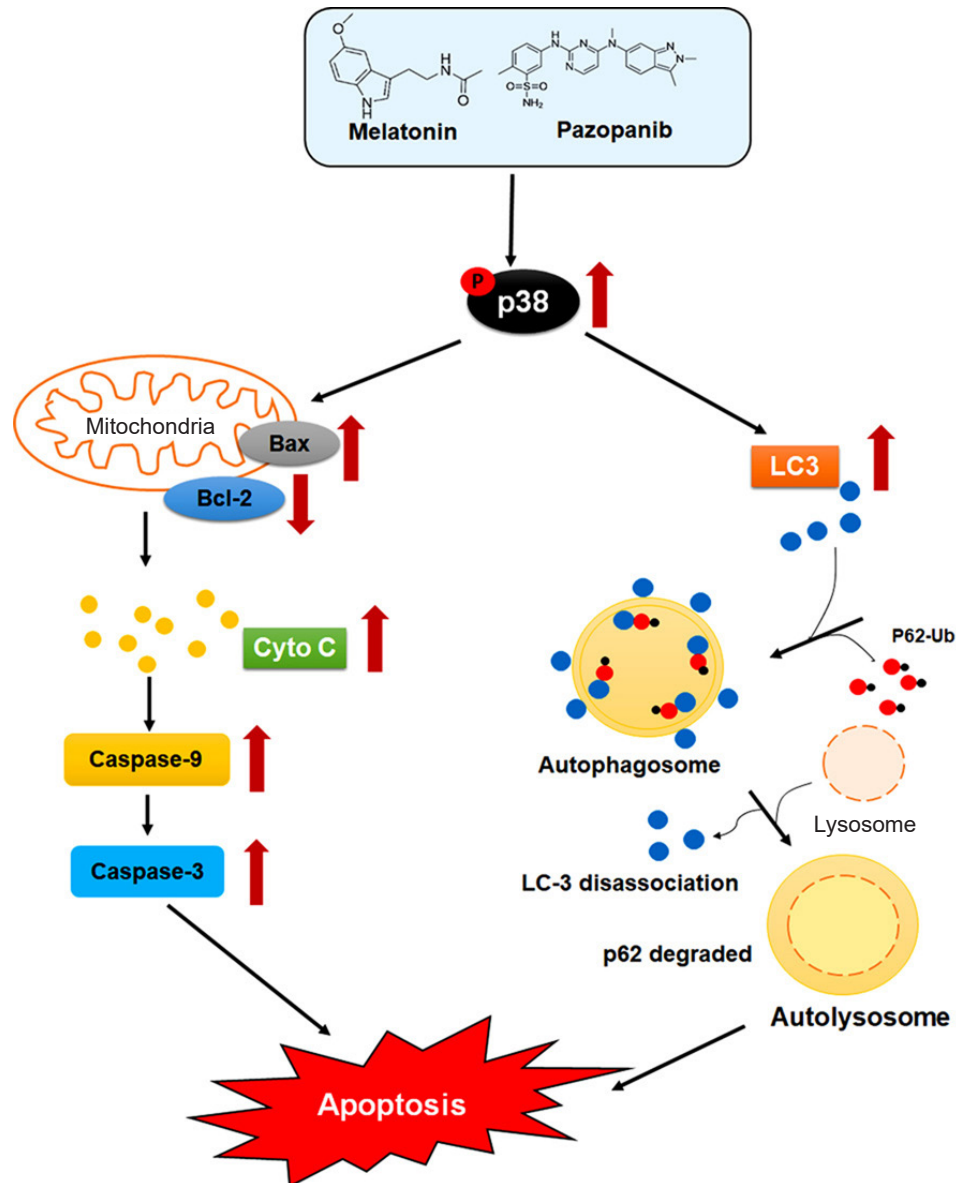


Figure 7. Proposed model for the antitumoral activity of melatonin combined with pazopanib against human RCC cells. The combination of melatonin and pazopanib induces p38MAPK activation, which subsequently triggers mitochondrial apoptotic signaling and autophagic signaling and thus leads to the apoptosis of RCC cells. RCC, renal cell carcinoma; p38MAPK, p38 mitogen-activated protein kinase.

the fibroblast growth factor receptor, and transmembrane glycoprotein RTKs [22]. Accordingly, pazopanib is used as the standard of care for patients with metastatic RCC. We used an *in vitro* cell model and found that pazopanib at the highest tested dose (10 μ M) exhibited a significant inhibitory effect on the viability of RCC cells. In contrast, pazopanib at the other tested doses (e.g., 5 μ M) showed negligible antitumor effects on RCC cells, including colony

formation, apoptosis, mitochondrial depolarization, and autophagy. Nonetheless, our *in vivo* results from a xenograft mouse model provide evidence that pazopanib significantly suppressed RCC tumor growth *in vivo*, consistent with clinical observations, even though it did not affect the tumorigenesis of RCC cells *in vitro*.

Currently, combination therapy aimed at multiple tumorigenic targets has emerged as a promising strategy to

reduce chemoresistance and improve the efficacy of tumor therapy. For example, the combination of the TKI sorafenib and the anti-interleukin-6R mAb tocilizumab can inhibit the angiogenesis and tumor growth of 786-O cells *in vivo* via the AKT/mTOR cascade more effectively than sorafenib alone [9]. In the past decade, melatonin has been increasingly demonstrated to be a potential antitumor compound or adjuvant for use with clinical anticancer drugs against several types of carcinoma cells, including osteosarcoma [23], thyroid cancer [24], gastric cancer [25], and colorectal cancer [26]. Our findings in this study reveal that melatonin combined with pazopanib significantly improved the antitumor activity of pazopanib monotherapy against RCC cells both *in vitro* and *in vivo*, and we have elucidated the mechanistic pathways affected by the combination treatment. Accordingly, we suggest that the combination of melatonin and pazopanib could be a potential therapy for metastatic RCC.

Mechanically, vascular endothelial growth factor triggers the activation of VEGFR2 through the autophosphorylation of tyrosine, subsequently recruiting phosphotyrosine binding proteins to induce downstream signaling cascades, such as the extracellular signal-regulated kinase, p38MAPK, PI3K/Akt, focal adhesion kinase, and Rho family GTPase pathways, which are all involved in the regulation of angiogenesis or vascular permeability [27]. Among those signaling components, the p38MAPK signaling induced by melatonin has been highly associated with multiple antitumor activities, including the suppression of matrix metalloproteinase-13 expression in prostate cancer cells [28] and the induction of G1 phase arrest and apoptosis in gastric cancer cells [29]. In contrast, p38MAPK inhibition in response to melatonin has also been reported to play important roles in reducing the stemness of lung cancer cells [30] and attenuating the migration of colon cancer cells [31]. Our findings show that melatonin, but not pazopanib, clearly induced p38MAPK phosphorylation, and the combination of melatonin and pazopanib triggered more p38MAPK phosphorylation than melatonin alone. These contradictory observations could reflect the different tumorigenic features of different carcinoma types.

The activation of apoptosis and autophagy is the primary antitumor effect of melatonin [32]. Consistently, our results show that melatonin and the combination of melatonin and low-dose pazopanib (5 μ M) induced mitochondrial

and autophagic apoptosis in RCC cells, which could explain the imbalance of Bax/Bcl-2, release of cytochrome c, activation of the caspase cascade, and upregulation of LC3-II we found, possibly via direct interactions of melatonin/LC3 and pazopanib/LC3. Interestingly, low-dose pazopanib alone did not affect apoptosis, mitochondrial depolarization, the Bax/Bcl-2 ratio, cytochrome c release, or LC3-II expression in RCC cells. Therefore, the efficacy of melatonin combined with low-dose pazopanib in the treatment of RCC might be similar to that of conventional chemotherapy, but with alleviated side effects.

Conflicts of interest

All authors have no conflicts of interest to declare.

Funding

This research was funded by the Chung-Kang Branch of the Cheng Ching General Hospital Research Fund (CH11100268A).

Data sharing statement

The data presented in this study are available on request from the corresponding author.

Authors' contributions

Conceptualization, Funding acquisition: CPL, THY, SHK, YHH

Data curation, Methodology: YSC, CYK

Formal analysis: YSC

Investigation: YSC, HLC, SHK, YHH

Project administration: THY, CYK, HLC, SHK

Writing–original draft: SHK, YHH

Writing–review & editing: CPL, SHK, YHH

All authors read and approved the final manuscript.

ORCID

Chien-Pin Lai, <https://orcid.org/0000-0002-5291-0108>

Yong-Syuan Chen, <https://orcid.org/0000-0001-5046-2594>

Tsung-Ho Ying, <https://orcid.org/0000-0001-8244-7524>

Cheng-Yen Kao, <https://orcid.org/0000-0003-1431-2956>

Hui-Ling Chiou, <https://orcid.org/0000-0001-5495-2224>
 Shao-Hsuan Kao, <https://orcid.org/0000-0002-4929-3858>
 Yi-Hsien Hsieh, <https://orcid.org/0000-0003-4942-1888>

References

- Gibbons RP, Monte JE, Correa RJ Jr, Mason JT. Manifestations of renal cell carcinoma. *Urology* 1976;8:201–206.
- Cohen HT, McGovern FJ. Renal-cell carcinoma. *N Engl J Med* 2005;353:2477–2490.
- Patard JJ, Leray E, Rioux-Leclercq N, et al. Prognostic value of histologic subtypes in renal cell carcinoma: a multicenter experience. *J Clin Oncol* 2005;23:2763–2771.
- Janzen NK, Kim HL, Figlin RA, Beldegrun AS. Surveillance after radical or partial nephrectomy for localized renal cell carcinoma and management of recurrent disease. *Urol Clin North Am* 2003;30:843–852.
- Gandaglia G, Ravi P, Abdollah F, et al. Contemporary incidence and mortality rates of kidney cancer in the United States. *Can Urol Assoc J* 2014;8:247–252.
- Ku X, Heinzlmeir S, Helm D, Médard G, Kuster B. New affinity probe targeting VEGF receptors for kinase inhibitor selectivity profiling by chemical proteomics. *J Proteome Res* 2014;13:2445–2452.
- Noujaim J, Payne LS, Judson I, Jones RL, Huang PH. Phosphoproteomics in translational research: a sarcoma perspective. *Ann Oncol* 2016;27:787–794.
- Canter D, Kutikov A, Golovine K, et al. Are all multi-targeted tyrosine kinase inhibitors created equal?: an in vitro study of sunitinib and pazopanib in renal cell carcinoma cell lines. *Can J Urol* 2011;18:5819–5825.
- Ishibashi K, Haber T, Breuksch I, et al. Overriding TKI resistance of renal cell carcinoma by combination therapy with IL-6 receptor blockade. *Oncotarget* 2017;8:55230–55245.
- von Gall C. The effects of light and the circadian system on rhythmic brain function. *Int J Mol Sci* 2022;23:2778.
- Cutando A, López-Valverde A, Arias-Santiago S, DE Vicente J, DE Diego RG. Role of melatonin in cancer treatment. *Anticancer Res* 2012;32:2747–2753.
- Luchetti F, Canonico B, Betti M, et al. Melatonin signaling and cell protection function. *FASEB J* 2010;24:3603–3624.
- Sanchez-Barcelo EJ, Mediavilla MD, Alonso-Gonzalez C, Reiter RJ. Melatonin uses in oncology: breast cancer prevention and reduction of the side effects of chemotherapy and radiation. *Expert Opin Investig Drugs* 2012;21:819–831.
- Tai HC, Wang SW, Swain S, et al. Melatonin suppresses the metastatic potential of osteoblastic prostate cancers by inhibiting integrin $\alpha 2 \beta 1$ expression. *J Pineal Res* 2022;72:e12793.
- Talib WH. A ketogenic diet combined with melatonin overcomes cisplatin and vincristine drug resistance in breast carcinoma syngraft. *Nutrition* 2020;72:110659.
- Odeh LH, Talib WH, Basheti IA. Synergistic effect of thymoquinone and melatonin against breast cancer implanted in mice. *J Cancer Res Ther* 2018;14:S324–S330.
- Lin CS, Lin CL, Ying TH, et al. β -Mangostin inhibits the metastatic power of cervical cancer cells attributing to suppression of JNK2/AP-1/Snail cascade. *J Cell Physiol* 2020;235:8446–8460.
- Kuo TN, Lin CS, Li GD, Kuo CY, Kao SH. Sesamin inhibits cervical cancer cell proliferation by promoting p53/PTEN-mediated apoptosis. *Int J Med Sci* 2020;17:2292–2298.
- Kawamura H, Li X, Goishi K, et al. Neuropilin-1 in regulation of VEGF-induced activation of p38MAPK and endothelial cell organization. *Blood* 2008;112:3638–3649.
- Park J, Jiao X, Ghate S, Wilson T, Ahmad QI, Vogelzang NJ. Predictors of long-term response with pazopanib in patients with advanced renal-cell carcinoma. *Clin Genitourin Cancer* 2018;16:293–297.
- Tullemans BM, Nagy M, Sabrkhany S, et al. Tyrosine kinase inhibitor pazopanib inhibits platelet procoagulant activity in renal cell carcinoma patients. *Front Cardiovasc Med* 2018;5:142.
- Gupta S, Spiess PE. The prospects of pazopanib in advanced renal cell carcinoma. *Ther Adv Urol* 2013;5:223–232.
- Li Y, Zou J, Li B, Du J. Anticancer effects of melatonin via regulating lncRNA JPX-Wnt/ β -catenin signalling pathway in human osteosarcoma cells. *J Cell Mol Med* 2021;25:9543–9556.
- Jia H, Sun W, Li X, Xu W. Melatonin promotes apoptosis of thyroid cancer cells via regulating the signaling of microRNA-21 (miR-21) and microRNA-30e (miR-30e). *Bioengineered* 2022;13:9588–9601.
- Li W, Hu C, Zhong X, Wu J, Li G. Melatonin induces AGS gastric cancer cell apoptosis via regulating PERK/eIF2 α and HSF1/NF- κ B signaling pathway. *Ann Clin Lab Sci* 2022;52:40–47.
- Zhao Y, Wang C, Goel A. A combined treatment with melatonin and andrographis promotes autophagy and anticancer activity in colorectal cancer. *Carcinogenesis* 2022;43:217–230.
- Roskoski R Jr. Vascular endothelial growth factor (VEGF) and VEGF receptor inhibitors in the treatment of renal cell carcinomas. *Pharmacol Res* 2017;120:116–132.
- Wang SW, Tai HC, Tang CH, et al. Melatonin impedes prostate cancer metastasis by suppressing MMP-13 expression. *J Cell*

- Physiol* 2021;236:3979–3990.
29. Huang Y, Yuan K, Tang M, et al. Melatonin inhibiting the survival of human gastric cancer cells under ER stress involving autophagy and Ras-Raf-MAPK signalling. *J Cell Mol Med* 2021;25:1480–1492.
 30. Yang YC, Chiou PC, Chen PC, et al. Melatonin reduces lung cancer stemness through inhibiting of PLC, ERK, p38, β -catenin, and Twist pathways. *Environ Toxicol* 2019;34:203–209.
 31. Liu Z, Zou D, Yang X, et al. Melatonin inhibits colon cancer RKO cell migration by downregulating Rho-associated protein kinase expression via the p38/MAPK signaling pathway. *Mol Med Rep* 2017;16:9383–9392.
 32. Wang Z, Liu Y, Musa AE. Regulation of cell death mechanisms by melatonin: implications in cancer therapy. *Anticancer Agents Med Chem* 2022;22:2080–2090.